


BRIEF DEFINITIVE REPORT

B cells are sufficient to prime the dominant CD4⁺ Tfh response to *Plasmodium* infection

E. Nicole Arroyo and Marion Pepper 

CD4⁺ T follicular helper (Tfh) cells dominate the acute response to a blood-stage *Plasmodium* infection and provide signals to direct B cell differentiation and protective antibody expression. We studied antigen-specific CD4⁺ Tfh cells responding to *Plasmodium* infection in order to understand the generation and maintenance of the Tfh response. We discovered that a dominant, phenotypically stable, CXCR5⁺ Tfh population emerges within the first 4 d of infection and results in a CXCR5⁺ CCR7⁺ Tfh/central memory T cell response that persists well after parasite clearance. We also found that CD4⁺ T cell priming by B cells was both necessary and sufficient to generate this Tfh-dominant response, whereas priming by conventional dendritic cells was dispensable. This study provides important insights into the development of CD4⁺ Tfh cells during *Plasmodium* infection and highlights the heterogeneity of antigen-presenting cells involved in CD4⁺ T cell priming.

Introduction

Malaria, caused by *Plasmodium* parasites, continues to pose serious health threats to developing areas of the world, especially sub-Saharan Africa and Southeast Asia (World Health Organization, 2018). Antibody production is critical for clearance of both human- and murine-tropic strains of the blood-stage parasite (Cohen et al., 1961; Crompton et al., 2010; Hirunpetcharat et al., 1997; Moss et al., 2012; Riley et al., 1992). CD4⁺ T cells are an important component of this response based on their role in eliciting T cell-dependent antibodies (Langhorne et al., 1990; McDonald and Phillips, 1978). Several studies have demonstrated that the acute response to a blood-stage *Plasmodium* infection in both humans and mice is dominated by CD4⁺ T follicular helper (Tfh) cells that provide help to B cells (Hahn et al., 2018; Obeng-Adjei et al., 2015; Pérez-Mazliah et al., 2015). However, it remains unknown how an endogenous antigen-specific Tfh population induced by *Plasmodium* infection forms or differentiates into a memory pool. Unlike in humans (Tran et al., 2013), acute *Plasmodium* infection in mice results in sterile immunity to reinfection initiated soon after the primary infection (Murphy, 1980). However, this period of sterilizing immunity to blood-stage parasites in mice is not life-long (Freitas do Rosário et al., 2008; Murphy, 1980); this raises questions about the formation and maintenance of memory cells in this model, which could illuminate failures of the human memory response to malaria. We developed a system to interrogate the development of the CD4⁺ memory T cell response to *Plasmodium* infection in mice with the hopes of gaining insights to enhance human immunity by vaccination.

Analysis of the expression of cell surface markers and fate-determining transcription factors by CD4⁺ T cells during *Plasmodium* infection demonstrates that the CD4⁺ T cell response is skewed to the Tfh phenotype (broadly defined as CXCR5⁺ BCL6⁺) as described in both humans and mice (Hahn et al., 2018; Obeng-Adjei et al., 2015; Pérez-Mazliah et al., 2015). Tfh cells interact with activated B cells at the T-B border between B cell follicles and T cell zones in lymphoid tissues and can develop into germinal center (GC) Tfh cells (CXCR5⁺ PD-1⁺; Haynes et al., 2007; Qi et al., 2008). Endogenous, epitope-specific polyclonal cells responding to either bacterial or viral infections tend to generate similar proportions of Tfh cells and non-Tfh T effector (Teff) cells at the population level due to heterogeneity within the naive CD4⁺ T cell repertoire (Tubo et al., 2013). This division of labor is evident within the first 5–10 d after infection and is thought to be driven initially by dendritic cell (DC) priming, followed by interactions with B cells (Hale et al., 2013; Pepper et al., 2011). Studies in bacterial and viral infections have also demonstrated that the Tfh population can then seed a CD4⁺ central memory T (T_{CM}) cell population (CCR7⁺ CXCR5⁺), which can reactivate in secondary challenges to express cytokines and help B cells (DiToro et al., 2018; Fairfax et al., 2015; Pepper et al., 2011). It is unclear why *Plasmodium* infection generates a dominant (~90%) Tfh response and how this skewing relates to memory formation of the antigen-specific cells (Freitas do Rosário et al., 2008). To this end, we studied the development of *Plasmodium*-specific CD4⁺ T cells and the factors influencing their differentiation.

Department of Immunology, University of Washington School of Medicine, Seattle, WA.

Correspondence to Marion Pepper: mpepper@uw.edu.

© 2019 Arroyo and Pepper. This article is distributed under the terms of an Attribution–Noncommercial–Share Alike–No Mirror Sites license for the first six months after the publication date (see <http://www.rupress.org/terms/>). After six months it is available under a Creative Commons License (Attribution–Noncommercial–Share Alike 4.0 International license, as described at <https://creativecommons.org/licenses/by-nc-sa/4.0/>).

We used a transgenic *Plasmodium yoelii* parasite that expresses a peptide from the lymphocytic choriomeningitis virus (LCMV) to compare GP66-specific (GP66⁺) CD4⁺ T cells in the context of *Plasmodium* or LCMV infection. This allowed us to compare the kinetics and differentiation of a single epitope-specific population with the same TCR repertoire responding to different infections. Recent work argues that within a polyclonal CD4⁺ T cell population, TCR affinity and signal strength strongly dictate the differentiation of Tfh cells (Keck et al., 2014; Knowlden and Sant, 2016; Krishnamoorthy et al., 2017; Tubo et al., 2013). Our approach interrogated the impact of distinct priming environments on directing the differentiation of the same epitope-specific population within different contexts. We found that GP66⁺ CD4⁺ T cells responding to *Plasmodium* infection exhibited reduced proliferative capacity compared with GP66⁺ cells responding to viral infection. Furthermore, we confirmed not only that a significant Tfh population arose at the peak of the response to *Plasmodium* (Pérez-Mazliah et al., 2015) but also that >80% of the CD4⁺ T cells exhibited a Tfh phenotype as early as 4 d after infection, suggesting an altered priming environment in response to *Plasmodium*. Further investigation revealed that while DCs were not required for the priming or differentiation of the CD4⁺ T cells during *Plasmodium* infection, B cells were both necessary and sufficient. We showed that both antigen presentation by B cells and T cell interpretation of costimulatory signals independently contributed to the expansion and differentiation of the GP66⁺ Tfh response, respectively. These studies challenge the paradigm that CD4⁺ T cells must first be primed by DCs before interacting with a B cell and suggest that in addition to TCR affinity and antigen load, the APC that primes the CD4⁺ T cell can influence its differentiation.

Results and discussion

Epitope-specific CD4⁺ T cells exhibit limited expansion in response to *Plasmodium* infection

To study an antigen-specific CD4⁺ T cell response to *P. yoelii* infection, we used a transgenic parasite expressing a well-characterized CD4⁺ T cell epitope derived from the GP of LCMV, GP₆₆₋₈₀ (Py-GP66; Dow et al., 2008; Hahn et al., 2018; Zander et al., 2017). This allowed us to use the previously generated GP₆₆₋₇₇:I-Ab tetramer and magnetic bead enrichment to examine rare, antigen-specific cells responding early in infection (Moon et al., 2007). To gain an understanding of the kinetics of the response, we first compared GP66⁺ cells in LCMV and Py-GP66 infections at various time points (Fig. 1, A and B). Comparable numbers of CD44⁺ GP66⁺ cells emerged from the naive precursor population of ~100 cells as early as 4 d after infection with either Py-GP66 or LCMV. However, whereas this reached a peak of ~4,000 cells at 12 d after infection with Py-GP66, it expanded to ~80,000 cells 12 d after LCMV infection, consistent with previous reports (MacLeod et al., 2008; Nelson et al., 2015; Whitmire et al., 2006; Fig. 1 B). Furthermore, in LCMV, the numbers of GP66⁺ cells contracted with viral clearance and then stabilized to maintain a population of long-lived memory cells, as previously described (Corbo-Rodgers et al., 2012; Hondowicz et al., 2018; Matloubian et al., 1994).

During *Plasmodium* infection, however, the number of CD44⁺ GP66⁺ cells continued to decline (Fig. 1 B). We analyzed the contraction of GP66⁺ cells from the peak at 12 d after infection to 150 d after infection by nonlinear regression (dashed lines). The slopes of the lines (31.15 for LCMV and -7.001 for Py-GP66) demonstrate that the contraction/memory phases have statistically different kinetics. As these differences begin early in the induction of the adaptive immune responses to these infections, we sought to examine how early events during the initiation of the GP66⁺ response may differentially impact the resulting expansion and maintenance of the cells.

Differences in the number of GP66⁺ cells in the two infections could arise due to multiple factors that affect how antigen is perceived at these early time points. Changes in antigen load can alter clonal expansion and the degree of T cell contraction (Park et al., 2008); differences in TCR signal strength can alter the transcriptional events downstream of TCR stimulation (Iwata et al., 2017); and alterations in costimulatory signals can sustain the proliferative burst (Howland et al., 2000; McAdam et al., 2000). T cell responsiveness during priming can be compared by measuring the responder frequency and proliferative capacity, which are associated with the perception of antigen and the maintenance of the proliferative burst (Gudmundsdottir et al., 1999). To address these possibilities, we adoptively transferred CFSE-labeled TCR transgenic CD4⁺ T cells specific for the GP66 epitope (SMARTA; Oxenius et al., 1998) into congenically marked WT recipients infected with LCMV or Py-GP66 1 d after transfer. We found that in both infections, GP66⁺ SMARTA cells undergo at least seven rounds of proliferation based on the dilution of CFSE (Fig. 1 C). We calculated both the responder frequency (the fraction of input SMARTA cells that proliferated at least once) and the proliferative capacity (the number of daughter cells generated per input SMARTA precursor cell; Gudmundsdottir et al., 1999). There was no difference in the responder frequency between the LCMV and Py-GP66 infections, indicating comparable access to antigen in both infections. However, there was a marked decrease in the proliferative capacity of the GP66⁺ SMARTA cells during *Plasmodium* infection, suggesting differential interpretation of costimulation (Fig. 1 D). These data demonstrate that the conditions required to sustain cell division, which can also influence cell fate, may be altered at an early stage in response to a *Plasmodium* infection.

Epitope-specific CD4⁺ T cells express CXCR5 at both acute and memory time points after infection

To gain a greater understanding of how the differentiation of these two epitope-specific populations occurs, we also examined the phenotype of the GP66⁺ CD4⁺ T cells in the context of the two infections. Current models suggest that a two-step process initiated by priming via a DC followed by subsequent interactions with B cells results in Tfh cell differentiation (Lu et al., 2011; Poholek et al., 2010). The initial interactions between DCs and CD4⁺ T cells are thought to drive an early bifurcation of activated CD4⁺ T cells into a Tfh or Teff pathway based on their ability to express CXCR5 or the IL-2R α chain, respectively (Chang et al., 2014; Pepper et al., 2011; Tubo et al., 2013). Tfh cells that

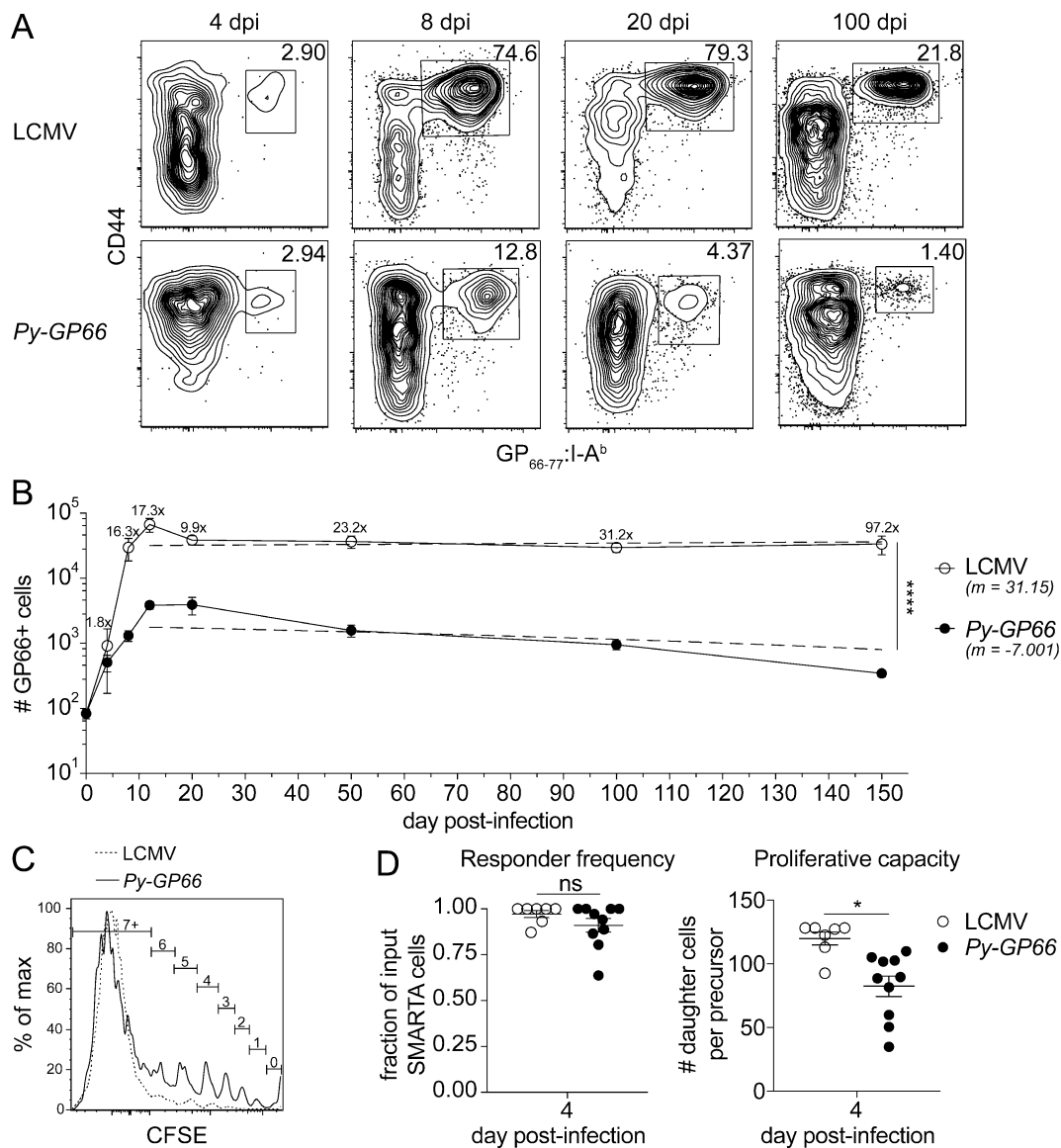


Figure 1. Epitope-specific CD4⁺ T cells exhibit limited expansion in response to *Plasmodium* infection. (A) At acute and late time points after infection with LCMV or *Py-GP66*, the activation and expansion of GP66⁺ CD4⁺ T cells from secondary lymphoid organs were assessed by flow cytometry. Plots are gated on dump⁻ CD3⁺ CD8⁻ CD4⁺ cells. **(B)** Graph shows the number of GP66⁺ cells from both infections over time. The fold change in the cell number from *Py-GP66* infection is indicated above the LCMV curve. Data are pooled from four to eight mice from each cohort at each time point from at least two independent experiments. A nonlinear regression from the peak at day 12 to day 150 was performed for each infection and is indicated by the dashed lines. The slope of the *Py-GP66* line is -7.001 (-17.75 to 3.747), and the slope of the LCMV line is 31.15 (-170.7 to 233). The regressions were analyzed by *F* test. **(C)** CFSE-labeled GP66-specific transgenic CD4⁺ T cells (SMARTA) were transferred to WT mice and infected with LCMV or *Py-GP66*. Numbers of cell divisions are indicated on gates. Both histograms are gated on SMARTA⁺ CD44⁺ GP66⁺ T cells. **(D)** Responder frequency and proliferative capacity of SMARTA⁺ CD44⁺ GP66⁺ cells were calculated as previously described (Gudmundsdottir et al., 1999). Data are pooled from 7–10 mice per cohort from two independent experiments and were analyzed by unpaired *t* test. For B and D, data are shown as means \pm SEM. *, $P < 0.05$; ****, $P < 0.0001$. dpi, days post-infection; ns, not significant.

upregulate BCL6 and CXCR5 migrate to the T–B border of secondary lymphoid organs where the Tfh phenotype is maintained by interactions with B cells (Cannons et al., 2010; Choi et al., 2011; Deenick et al., 2010; Glatman Zaretsky et al., 2009; Haynes et al., 2007; Johnston et al., 2009; Nurieva et al., 2008; Nurieva et al., 2009; Poholek et al., 2010; Qi et al., 2008; Salek-Ardakani et al., 2011; Watanabe et al., 2017).

We therefore first determined the kinetics of activated (CD44⁺) GP66⁺ CD4⁺ T cell differentiation in the two infections to understand how early the Tfh phenotype emerges. In

uninfected animals, GP66⁺ cells did not express CXCR5, as expected (Fig. 2 A; Tubo et al., 2013). At 4 d after infection, we could consistently find an expanded population of GP66⁺ cells in both infections. In LCMV-infected mice, only a small proportion of GP66⁺ cells expressed CXCR5 at this time point; yet the vast majority (~80%) of GP66⁺ cells responding to *Plasmodium* already expressed CXCR5 (Fig. 2 A). The global CD44⁺ CD4⁺ T cell population exhibits similarly enhanced Tfh skewing in response to *Plasmodium* infection compared with LCMV infection (Fig. S1, A and B). Approximately half of the cells responding to LCMV

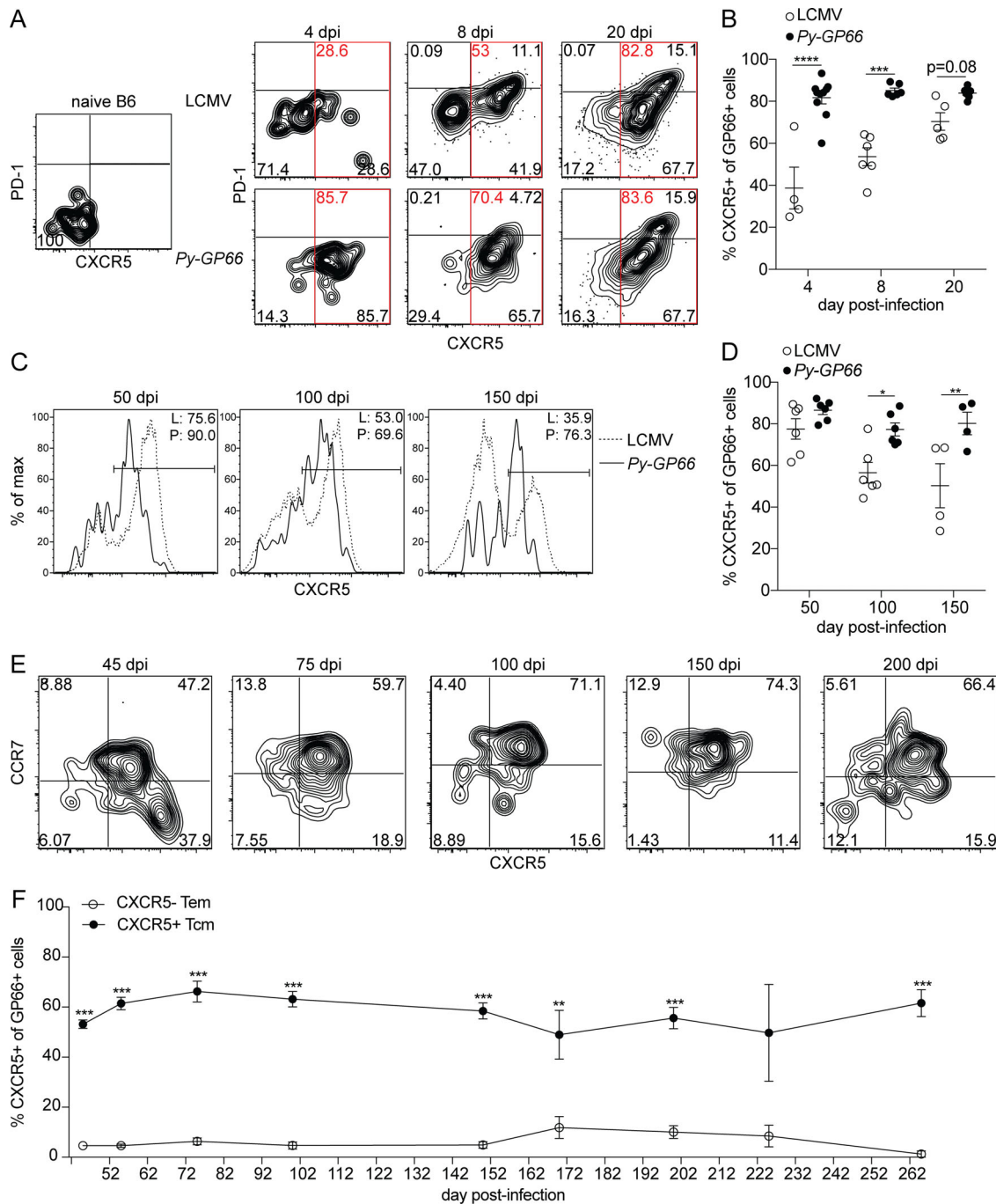


Figure 2. Epitope-specific CD4⁺ T cells express CXCR5 at both acute and memory time points after infection. (A) Representative flow plots of antigen-specific CD4⁺ T cells isolated from secondary lymphoid organs at naive or acute time points after LCMV or *Py-GP66* infection. Plots are gated on dump⁻ CD3⁺ CD8⁻ CD4⁺ CD44⁺ GP66⁺ cells. **(B)** Summary data of the percentage of CXCR5⁺ GP66⁺ cells shown in A (denoted by red gates). This quantification method for total CXCR5⁺ cells, including Tfh and GC Tfh at acute time points and CXCR5⁺ T_{CM} at later time points, is used throughout the paper. Data are pooled from four to eight mice per time point from at least two independent experiments and were analyzed by two-way ANOVA. **(C)** Representative flow plots of GP66-specific CD4⁺ T cells at memory time points after LCMV (L) or *Py-GP66* (P) infection. Frequencies of CXCR5⁺ cells are indicated in the plots. **(D)** Summary data of the percentage of CXCR5⁺ GP66⁺ cells shown in C. Data are pooled from four to six mice per time point from at least two independent experiments and were analyzed by two-way ANOVA. **(E)** Representative flow plots from GP66⁺ CD4⁺ T cells at memory time points after *Py-GP66*. CCR7⁺ T_{CM} cells and CCR7⁻ T_{EM} populations are shown. GC Tfh cells are included in the CCR7⁻ CXCR5⁺ population (Haynes et al., 2007). **(F)** Summary data of the percentage of the T_{CM} and the T_{EM} populations from E. Data are pooled from 3 to 10 mice per time point from at least two independent experiments and were analyzed by unpaired t test. For B, D, and F, data are shown as means ± SEM. *, P < 0.05; **, P < 0.01; ***, P < 0.001; ****, P < 0.0001. dpi, days post-infection.

exhibited a Tfh phenotype by day 8, as previously described (Tubo et al., 2013; Wu et al., 2015), though the frequency of CXCR5⁺ GP66⁺ cells continued to increase until day 20. In contrast, GP66⁺ cells induced by *Plasmodium* infection maintained a predominant CXCR5⁺ Tfh phenotype at all time points observed (Fig. 2, A and B). We confirmed that the CXCR5⁺ cells formed in *Plasmodium* infection were bona fide Th1 Tfh cells through analysis of the fate-determining transcription factors for this subset, T-bet and BCL6 (Cannons et al., 2010). While it was difficult to perform these studies on the low numbers of GP66⁺ cells at day 4, by day 8 after infection with *Plasmodium*, the majority of GP66⁺ cells expressed high levels of BCL6 and lower levels of T-bet, consistent with a Th1 Tfh phenotype (Fig. S1, C and D; Obeng-Adjei et al., 2015). Together, these data demonstrate that the same epitope-specific population can adopt different frequencies of Tfh versus T_{eff} phenotypes with different kinetics in response to different infections. These data further suggest that some aspect of *Plasmodium* infection commits the GP66⁺ cells to a stable Tfh phenotype very early in infection.

We next assessed the stability of this early Tfh population by analyzing the GP66⁺ cells at later time points. We hypothesized that the early Tfh cell differentiation would later result in a central memory population, as previously described in Th1 cell-skewed responses to bacterial and viral infections (DiToro et al., 2018; Pepper et al., 2011). 50 d after either infection, the majority of GP66⁺ cells maintained a CXCR5⁺ Tfh phenotype; however, at later time points, the frequency of CXCR5⁺ cells decreased in the LCMV-infected mice, while *Plasmodium*-infected mice maintained ~80% CXCR5⁺ cells (Fig. 2, C and D). Of note, the level of CXCR5 expression, as determined by mean fluorescence intensity, on the GP66⁺ cells after LCMV infection was consistently higher than after *Plasmodium* infection at all the time points tested, despite the frequency of total CXCR5⁺ cells being generally higher in response to *Plasmodium* infection than to LCMV infection (Fig. 2, C and D).

To determine the types of memory cells that form in response to *Plasmodium* infection, we also assessed markers that distinguish central and effector memory cells (CCR7 and CD62L; Sallusto et al., 1999). Gates were drawn using the expression of CCR7 and CXCR5 on global CD4⁺ T cells and CD44⁺ CD4⁺ T cells (Fig. S1 E). We demonstrated that GP66⁺ memory T cells following *Plasmodium* infection largely adopted a T_{CM} (CCR7⁺ CXCR5⁺) phenotype (Fig. 2 E). This skewing in the memory pool was observed at all time points examined up to 260 d after infection (Fig. 2 F). These data therefore demonstrate that the early differentiation of CXCR5⁺ Tfh cells observed was maintained as a CXCR5⁺ T_{CM} cell population, suggesting that this is a stable phenotype, imprinted early in the response to *Plasmodium* infection.

The Tfh-skewed epitope-specific CD4⁺ T cell response is B cell dependent

We next focused on understanding the factors that could be driving this stable CXCR5⁺ Tfh/T_{CM}-skewed phenotype. As described above, Tfh cell differentiation is thought to be a two-step process depending on early priming by DCs and later maintenance of the Tfh phenotype by B cells. We therefore

hypothesized that CD4⁺ T cells activated in the absence of B cells would show no phenotypic differences at day 4 but would fail to maintain the Tfh phenotype later. We tested this hypothesis by infecting WT and μ MT mice, which lack mature B cells, with *Py-GP66* and examined the phenotype of GP66⁺ cells in each group at various time points. Interestingly, we observed that even as early as 4 d after infection there was a significant loss of CXCR5 expression by GP66⁺ cells in the μ MT mice (Fig. 3 A). Later, a small population of Tfh cells emerged, which was consistently half as frequent in the μ MT mice as in the WT mice (Fig. 3, A and B). Although the exact kinetics of cell expansion in this experiment differed from the more extensive analyses shown in Fig. 1 B due to the biological variation associated with infection, the number of GP66⁺ cells was consistently lower in μ MT mice than in WT mice during the acute response to *Plasmodium* infection (Fig. 3 B). These data suggest that B cells play a crucial role in the CD4⁺ T cell response to *Plasmodium* infection before day 4. We were unable to study these cells beyond day 15 due to fatality in the μ MT mice resulting from a high parasite burden (Fig. S2 A; Roberts et al., 1977; Weinbaum et al., 1976). Since μ MT animals are known to have aberrant lymphoid organization (Chyou et al., 2011), we also depleted B cells in WT mice with anti-CD20 antibody administered on the day of and 3 d after infection with *Py-GP66*. We achieved 81% reduction of B cells in the spleen with this treatment compared with the isotype-treated control (Fig. S2 B). At 4 d after infection, we observed that transient depletion of B cells decreased the Tfh population by ~20% compared with the isotype-treated control (Fig. 3, C and D). The B cell depletion resulted in a decreased number of GP66⁺ cells, though this was not significant (Fig. 3 D). These alterations in differentiation occurred without appreciable increases in the parasite burden compared with that of WT controls, suggesting no critical role for antibody production at early time points (Fig. S2, A and C). These data support our hypothesis that B cells are critical for providing very early signals in response to *Plasmodium* infection, and even partial depletion of B cells can affect the early differentiation of a predominant *Plasmodium*-specific Tfh response.

B cells are necessary and sufficient to prime the GP66⁺ CD4⁺ T cell response, while DCs are dispensable

CD4⁺ T cells interpret multiple signals from professional APCs during priming, including presentation of antigen on peptide-MHC complexes and ligand/receptor pair interactions, referred to as costimulation. Many reports indicate that DCs serve as the initial APC for Tfh cell differentiation in various infections (Barnett et al., 2014; Cassell and Schwartz, 1994; Deenick et al., 2010; Itano et al., 2003). Previous studies identified conventional DCs (cDCs) as the critical APC during *Plasmodium* infection (Fernandez-Ruiz et al., 2017; Ueffing et al., 2017; Voisine et al., 2010). However, these studies used CD11c as the cDC marker, which is also upregulated by activated B cells, CD4⁺ T cells, CD8⁺ T cells, natural killer (NK) cells, and NK T cells (Rubtsov et al., 2011; Satpathy et al., 2012; Sullivan et al., 2015; Weiss et al., 2009). In other studies, DCs have been shown to have dysfunctional responses during blood-stage *Plasmodium*, including a reduced capacity for antigen uptake and antigen presentation (Götz et al., 2017; Loughland et al., 2017; Pinzon-

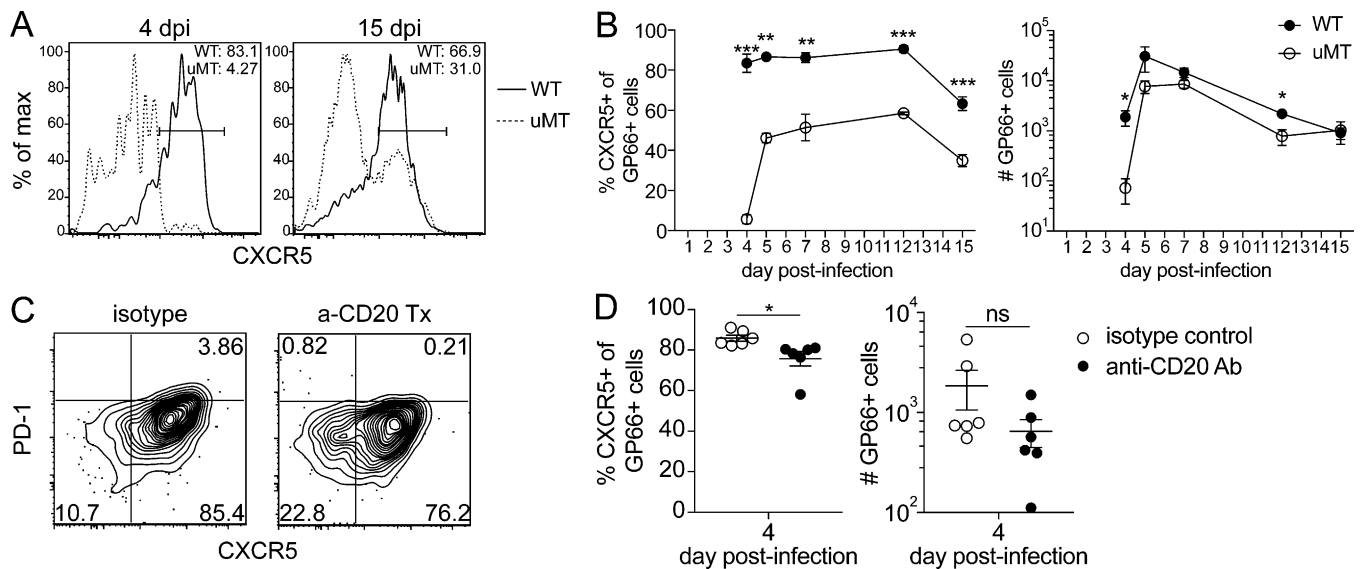


Figure 3. The Tfh-skewed epitope-specific CD4⁺ T cell response is B cell dependent. (A) Representative flow plots demonstrating CXCR5 expression on antigen-specific CD4⁺ T cells at acute time points after *Py-GP66* infection in WT and uMT mice. Plots are gated on dump⁻ CD3⁺ CD8⁻ CD4⁺ CD44⁺ GP66⁺ cells. (B) Summary data of the percentage of CXCR5⁺ GP66⁺ cells and number of GP66⁺ cells from A. Data are pooled from three to six mice per cohort from at least two independent experiments and were analyzed by unpaired *t* test. (C) WT mice were treated with anti-CD20 antibody or isotype control immediately before infection and on day 3 after infection. Representative flow plots of GP66⁺ cells from the secondary lymphoid organs of mice infected 4 d prior with *Py-GP66*. (D) Summary data of the percentage of CXCR5⁺ GP66⁺ cells and number of GP66⁺ cells from C. Data are pooled from six mice per cohort from two independent experiments and were analyzed by unpaired *t* test. For B and D, data are shown as means ± SEM. *, *P* < 0.05; **, *P* < 0.01; ***, *P* < 0.001. Ab, antibody; dpi, days post-infection; ns, not significant.

Charry et al., 2013; Urban et al., 1999; Woodberry et al., 2012; Wykes et al., 2007).

We therefore tested whether cDCs were involved in CD4⁺ T cell priming during *Plasmodium* infection using a more specific deletion of cDCs. We used the Zbtb46-DTR (zDC-DTR) mouse model, in which administration of diphtheria toxin specifically depletes the cDC compartment without affecting plasmacytoid DCs, macrophages, monocytes, or NK cells (Meredith et al., 2012). We achieved a 77% depletion of the cDC compartment in these mice 2 d after treatment (Fig. S3 A) and found that in the absence of cDCs, GP66⁺ cells maintain a prominent Tfh skewing at day 4 after infection (Fig. 4 A). Furthermore, we observed no significant changes in the frequency of CXCR5⁺ cells or the number of GP66⁺ cells (Fig. 4 B). Together, these data demonstrate that cDCs are not necessary to activate *Plasmodium*-specific CD4⁺ T cells or to promote Tfh cell differentiation in the context of this infection. Our approach allows for the dissection of the specific contribution of the cDCs and demonstrates that they are dispensable for activation of *Plasmodium*-specific CD4⁺ T cells.

We next examined whether, alternatively, B cells could be priming CD4⁺ T cells in response to *Plasmodium* infection. Following activation, B cells upregulate MHC II and costimulatory molecules, demonstrating their capacity to prime naive CD4⁺ T cells (Barnett et al., 2014; Constant, 1999; Hawrylowicz and Unanue, 1988; Hong et al., 2018; Krieger et al., 1985). Additionally, B cell priming has been demonstrated *in vivo* using mice that only express MHC II (I-Ab) on CD19⁺ B cells (B-MHC II). In B-MHC II mice, antigen presentation by B cells was shown to be sufficient to drive the expansion and formation of antigen-

specific Tfh cells in response to immunization (Constant, 1999) and during viral infection (Barnett et al., 2014; Evans et al., 2000; Hong et al., 2018). We used these mice to determine whether a similar phenomenon could occur in response to *Plasmodium* infection. Since B-MHC II mice do not develop a normal CD4⁺ T cell compartment due to the lack of positive selection (Barnett et al., 2014), it is necessary to adoptively transfer CD4⁺ T cells and examine these. We transferred TCR transgenic SMARTA CD4⁺ T cells specific for the GP66 epitope into WT or B-MHC II mice 1 d before infection with LCMV or *Py-GP66* and analyzed the differentiation of these cells 4 d after infection. As expected, the absence of DC-derived priming hampered the expansion of GP66⁺ SMARTA cells responding to LCMV infection but did not impact expansion during *Plasmodium* infection. We observed a small decrease in the expression of CXCR5 at 4 d after infection when cells were responding to LCMV infection. Remarkably, in response to *Plasmodium* infection, the GP66⁺ SMARTA cells in B-MHC II mice developed a prominent Tfh skewing that closely resembled their phenotype in WT controls (Fig. 4, C and D).

To perform the converse experiment, we generated MB1-Cre⁺ MHC II^{fl/fl} mice to delete the β chain of the I-Ab MHC II molecule from B cells, thus preventing B cells from presenting antigen. 4 d after infection with *Py-GP66*, there was a 10% decrease in Tfh frequency and a sevenfold reduction in the total number of GP66⁺ cells generated in mice lacking MHC class II on B cells (Fig. 4, E and F). Together, these data demonstrate that B cells play a significant role in directing the expansion of CD4⁺ T cells responding to *Plasmodium* infection independently of DCs. These data also support more recent work demonstrating

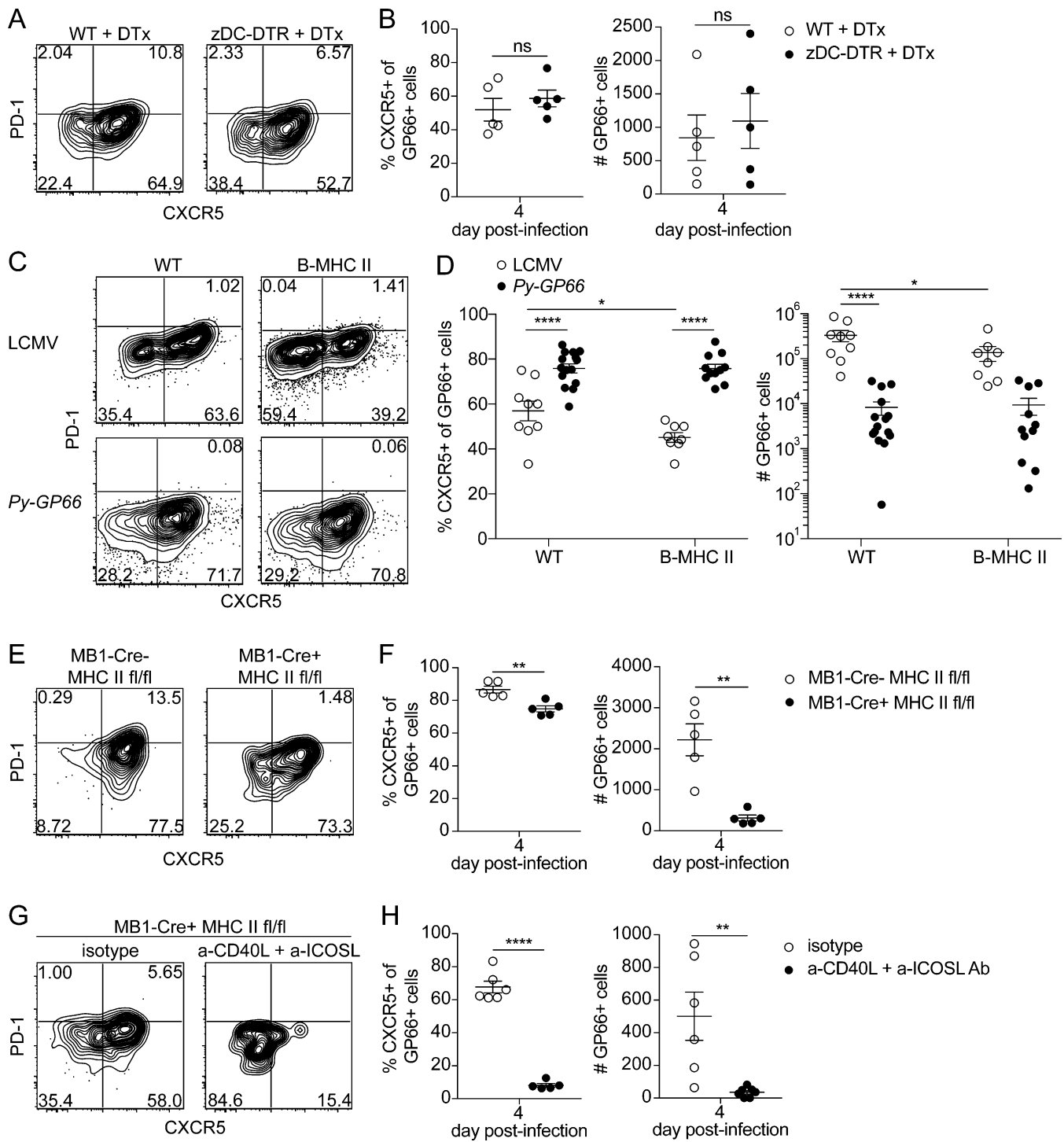


Figure 4. B cells are necessary and sufficient to prime the GP66⁺ CD4⁺ T cell response, whereas DCs are dispensable. (A) Representative flow plots of GP66⁺ cells from 4 d after infection with Py-GP66 in WT and zDC-DTR mice. Both cohorts were treated with diphtheria toxin (DTx) at 1 and 2 d after infection. (B) Summary data of the percentage of CXCR5⁺ GP66⁺ cells and number of GP66⁺ cells in A. Data are pooled from five mice per cohort and are representative of two independent experiments. Data were analyzed by unpaired *t* test. (C) Representative flow plots showing transferred SMARTA⁺ GP66⁺ cells 4 d after infection with LCMV or Py-GP66 in WT and B-MHC II mice. Plots are gated on dump⁻ CD3⁺ CD8⁻ CD4⁺ CD44⁺ GP66⁺ cells. (D) Summary data of the percentage of CXCR5⁺ SMARTA⁺ GP66⁺ cells and number of SMARTA⁺ GP66⁺ cells shown in C. Data are pooled from 8–15 mice per cohort and are representative of three independent experiments. Data were analyzed by two-way ANOVA. (E) Representative flow plots of endogenous GP66⁺ CD4⁺ T cells from MB1-Cre⁻ MHC^{fl/fl} or MB1-Cre⁺ MHC^{fl/fl} mice infected with Py-GP66 4 d prior. (F) Summary data of the percentage of CXCR5⁺ GP66⁺ cells and number of GP66⁺ cells shown in E. Data are representative of five mice per cohort from two independent experiments and were analyzed by unpaired *t* test. (G) MB1-Cre⁺ MHC^{fl/fl} mice were treated with a-CD40L + a-ICOSL antibodies or isotype controls daily 0–3 d after infection. Representative flow plots from GP66⁺ cells 4 d after infection with Py-GP66. (H) Summary data of the percentage of CXCR5⁺ GP66⁺ cells and number of GP66⁺ cells from G. Data are pooled from five or six mice per cohort and are representative of two independent experiments. Data were analyzed by unpaired *t* test. For B, D, F, and H, data are shown as means ± SEM. *, *P* < 0.05; **, *P* < 0.01; ****, *P* < 0.0001. ns, not significant.

that antigen presentation by B cells alone is sufficient to drive the expansion and formation of prominent Tfh populations in the context of infection (Hong et al., 2018).

Since B cells can influence the differentiation of CD4⁺ T cells through both antigen presentation and costimulation, we also interrogated how costimulatory signals influence the differentiation of the Tfh response to *Plasmodium* infection. B cells can provide an array of costimulatory signals, including CD40 and ICOSL, which are critical for driving the differentiation of Tfh cells (Cannons et al., 2010; Choi et al., 2011; Deenick et al., 2010; Glatman Zaretsky et al., 2009; Haynes et al., 2007; Johnston et al., 2009; Nurieva et al., 2008; Nurieva et al., 2009; Poholek et al., 2010; Qi et al., 2008; Salek-Ardakani et al., 2011; Watanabe et al., 2017). We therefore began by testing how CD40-CD40L and ICOS-ICOSL interactions direct the differentiation of GP66⁺ cells. We infected WT and MBI-Cre⁺ MHC II^{fl/fl} mice with Py-GP66, treated with anti-CD40L and anti-ICOSL antibodies daily for the first 3 d of infection, and analyzed the responses at 4 d after infection. Blocking interactions between these receptor-ligand pairs in WT mice resulted in a 12% decrease in CXCR5⁺ Tfh cells, as well as a 1.7-fold decrease in cell numbers (Fig. S3, B and C). When this treatment was conducted in MBI-Cre⁺ MHC II^{fl/fl} mice to determine if synergy might occur between antigen-dependent and -independent interactions, we observed a nearly 60% decrease in the frequency of CXCR5⁺ T cells, in addition to a 14-fold decrease in the total numbers of GP66⁺ cells (mean = 35.2 cells) compared with isotype-treated controls (Fig. 4, G and H). Independently, the effects of removing antigen presentation by B cells or blocking costimulation had notable effects on the differentiation of Tfh cells. However, the dramatic reductions in both Tfh cell differentiation and antigen-specific cell expansion when both antigen presentation and costimulatory interactions between CD4⁺ T cells and B cells were blocked highlights the synergy of the multiple cues that determine CD4⁺ T cell fate. These data emphasize the importance of both costimulation and antigen presentation for CD4⁺ T cell fate during the priming phase of the immune response to *Plasmodium* infection.

Conclusion

Our data support a model in which B cells serve as the primary APC during blood-stage *Plasmodium* infection. The distinctive role for B cells in this context is likely influenced by diminished DC function (Götz et al., 2017; Loughland et al., 2017; Pinzon-Charry et al., 2013; Urban et al., 1999; Woodberry et al., 2012; Wykes et al., 2007) and/or the splenic disruption associated with this infection (Cadman et al., 2008). The *Plasmodium*-specific CD4⁺ T cell population acquires a stable CXCR5⁺ Tfh phenotype at acute time points during infection that is maintained late into the memory response. As shown in previous bacterial and viral infections, this early Tfh cell population can form a prominent T_{CM} population (DiToro et al., 2018; Fairfax et al., 2015; Pepper et al., 2011). This is in contrast to other studies (Stephens and Langhorne, 2010; Opata et al., 2015) in which adoptively transferred, *Plasmodium*-specific monoclonal TCR transgenic CD4⁺ T cells predominantly formed an effector memory T (T_{EM}) cell population. This result may be due to the

specificity of the population that was used, as monoclonal TCR transgenic populations do not always represent the heterogeneity seen in polyclonal endogenous antigen-specific populations (Tubo et al., 2013).

This work demonstrates that B cells can provide both peptide-MHC complexes and costimulatory signals required for priming CD4⁺ T cells generated during *Plasmodium* infection. Of interest, several studies have noted an increase in the circulating cDC1 population in humans following *Plasmodium* infection, coupled with a significant decrease in the surface expression of the human MHC II molecule HLA-DR (Arama et al., 2011; Guermonprez et al., 2013; Urban et al., 2006). Many have reported a decrease in antigen uptake and presentation by DCs in both mouse and human studies (Götz et al., 2017; Loughland et al., 2017; Pinzon-Charry et al., 2013; Urban et al., 1999; Woodberry et al., 2012; Wykes et al., 2007). Others described a specific dysfunction of the cDCs to prime CD4⁺ T cells due to the type I IFN signaling induced early in infection (Haque et al., 2014). These findings together with our work support the hypothesis that while T cell-promoting cDCs are increased in number, they are significantly hampered in their functionality. This may result in the B cell population being the professional APC population poised to prime CD4⁺ T cells and promote Tfh formation.

Additionally, the architectural changes that have been described in the spleen during *Plasmodium* infection of both mice and humans are characterized by the presence of B cells outside the follicle and a blurring of the red and white pulp areas (Achtman et al., 2003; Alves et al., 2015; Cadman et al., 2008; Urban et al., 2005). We hypothesize that the loss of well-defined B and T cell areas allows CD4⁺ T and B cells to freely associate and exchange signals that would normally be provided only at the T-B border, resulting in depressed cell numbers and skewed Tfh cell differentiation early in the response to *Plasmodium* infection. While it is unclear whether the costimulatory signals required to form Tfh cells are provided by B cells, it is clear that cDCs are not critical for this function. Overall, the work here demonstrates that B cells play an important role early in the development of the CD4⁺ T cell response during *Plasmodium* infection before antibody production, through antigen presentation and likely costimulatory factors such as CD40 and ICOSL. Elucidating the comprehensive effects of early B cell interactions on acute CD4⁺ T cell responses and their effects on memory CD4⁺ T cell fate in the context of *Plasmodium* infection will provide the field with additional therapeutic targets to improve immunity to *Plasmodium* infection.

Materials and methods

Mice

4–10-wk-old male C57BL/6, B6.129S2-Ighmtm1Cgn/J (μMT), B6.C(Cg)-Cd79a^{tm1(cre)Reth}/EhobJ (MB1-Cre), and B6.129X1-H2-Ab1^{tm1Koni}/J (I-A^b fl/fl) mice were purchased from the Jackson Laboratory. MB1-Cre and I-A^b fl/fl mice were crossed to generate the MB1-Cre⁺ MHC II^{fl/fl} strain. MB1-Cre⁻ MHC II^{fl/fl} littermates were used as controls for these experiments. B6;D2-TCR LCMV RAG-deficient (SMARTA) mice were provided by Dr. James Moon (Massachusetts General Hospital, Harvard Medical

School, Boston, MA). CD19-A β b (B-MHC II) mice (Barnett et al., 2014) were provided by Dr. Terri Laufer (University of Pennsylvania, Philadelphia, PA). B6(Cg)-Zbtb46^{tm1(HBEGF)Mnz/J} (zDC-DTR) mice (Meredith et al., 2012) were provided by Dr. Michael Gerner (University of Washington, Seattle, WA). All animals were bred and housed under specific pathogen-free conditions at the University of Washington. Animals infected with LCMV were housed in Animal Biosafety Level-2 conditions. Experiments were performed in accordance with the University of Washington Institutional Animal Care and Use Committee guidelines.

Parasite and viral infections

P. yoelii 17XNL-GP66 (Py-GP66) parasites (Hahn et al., 2018; Zander et al., 2017) were maintained as frozen blood stocks and passaged through donor mice. Py-GP66 infections were initiated by an i.p. injection of 10⁶ infected RBCs per mouse obtained from donor mice. Parasitemia was determined by flow cytometry based on the percentage of CD45⁻ Ter119⁺ Hoescht⁺ cells (Malleret et al., 2011). LCMV-Armstrong strain was provided by Dr. David Masopust (University of Minnesota, Minneapolis, MN). LCMV infections were initiated by i.p. injection of 10⁵ PFU per mouse.

Purified antibody and diphtheria toxin treatments

For depletion of CD20⁺ B cells, mice were anesthetized with isoflurane and treated with anti-CD20 antibody (clone 18B12; generously provided by Biogen Idec) at 10 mg/kg in PBS via i.v. injection. Control mice were treated with 10 mg/kg of isotype control antibody (clone 2B8; Biogen Idec) in PBS via i.v. injection. Doses were administered at 0 and 3 d after infection, according to the depletion kinetics (Dunn et al., 2007). For the blockade of CD40-CD40L and ICOS-ICOSL signaling, mice were treated with 0.5 mg of anti-CD40L antibody (clone MR-1; Bio X Cell) and 0.25 mg of anti-ICOSL antibody (clone HK5.3; Bio X Cell) in PBS via i.v. injection daily from 0 to 3 d after infection. Control mice received 0.5 mg and/or 0.25 mg of polyclonal Armenian hamster IgG and rat IgG2, respectively (Bio X Cell). Diphtheria toxin (Sigma) was administered via i.p. injection at 20 ng/g at 1 d before infection and 2 d after infection.

SMARTA cell transfer

CD4⁺ T cells were isolated from SMARTA mice by negative selection with the CD4⁺ T cell MACS isolation kit (Miltenyi Biotec) and were labeled with CFSE (Invitrogen). Recipient mice were anesthetized with isoflurane and received 10⁵ CFSE-labeled CD4⁺ T cells via i.v. injection 1 d before infection.

Cell enrichment and flow cytometry

Single-cell suspensions were prepared from the spleen and lymph nodes (axial, brachial, cervical, inguinal, mesenteric, and periaortic) from experimental mice in PBS containing 2% heat-inactivated FBS. Cells were stained with GP₆₆₋₇₇:I-A^b-APC tetramer (I-A^b/LCMV.GP66.DIYKGVYQFKSV; National Institutes of Health Tetramer Core) for 1 h at room temperature, washed,

and incubated with magnetic anti-APC beads (Miltenyi Biotec) for 30 min on ice. Tetramer-specific cells were enriched as previously described (Moon et al., 2007) using LS MACS columns (Miltenyi Biotec). The enriched cells were stained with antibodies to the following surface markers: CCR7 (clone: 4B12; Biolegend or eBioscience), CD3 (clone: 145-2C11; BD), CD4 (clone: RM4-4, RM4-5, or GK1.5), CD8a (clone: 53-6.7; BD), CD11b (clone: M1/70; eBioscience or BD), CD11c (clone: N418; eBioscience; clone: HL3; BD), CD25 (clone: PC61; BD), CD44 (clone: IM7; BD), CD45R (B220) (clone: RA3-6B2; eBioscience or BD), CD62L (clone: MEL-14; BD), CD69 (clone: H1.2F3; eBioscience), CXCR5 (clone: 2G8; BD), F4/80 (clone: BM8; eBioscience), PD-1 (clone: J43; eBioscience), and streptavidin (BD). For intranuclear transcription factor staining, cells were then fixed with eBioscience Foxp3/Transcription Factor Staining Buffer Set (Thermo Fisher) and stained with antibodies to the following intranuclear molecules: BCL6 (clone: K112-91; BD) and T-bet (clone: eBio4B10; eBioscience). All samples were acquired on the LSR II cytometer (BD) and analyzed using FlowJo software (Tree Star, v9). All flow plots were gated on lymphocyte gate, singlets, B220⁻ CD11b⁻ CD11c⁻ (dump⁻) CD3⁺ CD8⁻ CD4⁺. Additional gating strategies are indicated in the figure legends.

Statistical analysis

Responder frequency and proliferative capacity were calculated as previously described (Gudmundsdottir et al., 1999). Results represent means \pm SEM. Statistical analyses were performed by nonlinear regression, unpaired *t* test, or two-way ANOVA, as specified in figure legends. Statistical tests were calculated using GraphPad Prism (v7).

Online supplemental material

Fig. S1 shows the expression of Tfh and T_{CM} markers in naive cells. Fig. S2 shows the impact of B cell loss on parasite burden and the depletion of B cells by anti-CD20 antibody treatment. Fig. S3 shows the depletion of cDCs and the loss of Tfh cells in WT mice in response to CD40L and ICOSL blockade.

Acknowledgments

Py-GP66 mosquito passage was generously performed by Alexis Kaushansky (Seattle Children's Research Institute, Seattle, WA). Terri Laufer provided valuable discussions and generously provided mice.

This work was supported by the National Institutes of Health (grant R01 AI108626-01A1), and E.N. Arroyo was supported by the National Institutes of Health training grants T32 AI106677-04 and T32 GM007270.

The authors declare no competing financial interests.

Author contributions: E.N. Arroyo designed the study, performed the experiments, analyzed the data, and wrote the manuscript. M. Pepper designed the study, analyzed the data, and wrote the manuscript.

Submitted: 10 May 2019

Revised: 19 August 2019

Accepted: 23 October 2019

References

- Achtman, A.H., M. Khan, I.C. MacLennan, and J. Langhorne. 2003. Plasmodium chabaudi chabaudi infection in mice induces strong B cell responses and striking but temporary changes in splenic cell distribution. *J. Immunol.* 171:317–324. <https://doi.org/10.4049/jimmunol.171.1.317>
- Alves, F.A., M. Pelajo-Machado, P.R. Totino, M.T. Souza, E.C. Gonçalves, M.P. Schneider, J.A. Muniz, M.A. Krieger, M.C. Andrade, C.T. Daniel-Ribeiro, and L.J. Carvalho. 2015. Splenic architecture disruption and parasite-induced splenocyte activation and anergy in Plasmodium falciparum-infected Saimiri sciureus monkeys. *Malar. J.* 14:128. <https://doi.org/10.1186/s12936-015-0641-3>
- Arama, C., P. Giusti, S. Boström, V. Dara, B. Traore, A. Dolo, O. Doumbo, S. Varani, and M. Troye-Blomberg. 2011. Interethnic differences in antigen-presenting cell activation and TLR responses in Malian children during Plasmodium falciparum malaria. *PLoS One.* 6:e18319. <https://doi.org/10.1371/journal.pone.0018319>
- Barnett, L.G., H.M. Simkins, B.E. Barnett, L.L. Korn, A.L. Johnson, E.J. Wherry, G.F. Wu, and T.M. Laufer. 2014. B cell antigen presentation in the initiation of follicular helper T cell and germinal center differentiation. *J. Immunol.* 192:3607–3617. <https://doi.org/10.4049/jimmunol.1301284>
- Cadman, E.T., A.Y. Abdallah, C. Voisine, A.M. Sponaas, P. Corran, T. Lamb, D. Brown, F. Ndungu, and J. Langhorne. 2008. Alterations of splenic architecture in malaria are induced independently of Toll-like receptors 2, 4, and 9 or MyD88 and may affect antibody affinity. *Infect. Immun.* 76:3924–3931. <https://doi.org/10.1128/IAI.00372-08>
- Cannons, J.L., H. Qi, K.T. Lu, M. Dutta, J. Gomez-Rodriguez, J. Cheng, E.K. Wakeland, R.N. Germain, and P.L. Schwartzberg. 2010. Optimal germinal center responses require a multistage T cell:B cell adhesion process involving integrins, SLAM-associated protein, and CD84. *Immunity.* 32:253–265. <https://doi.org/10.1016/j.immuni.2010.01.010>
- Cassell, D.J., and R.H. Schwartz. 1994. A quantitative analysis of antigen-presenting cell function: activated B cells stimulate naive CD4 T cells but are inferior to dendritic cells in providing costimulation. *J. Exp. Med.* 180:1829–1840. <https://doi.org/10.1084/jem.180.5.1829>
- Chang, J.T., E.J. Wherry, and A.W. Goldrath. 2014. Molecular regulation of effector and memory T cell differentiation. *Nat. Immunol.* 15:1104–1115. <https://doi.org/10.1038/ni.3031>
- Choi, Y.S., R. Kageyama, D. Eto, T.C. Escobar, R.J. Johnston, L. Monticelli, C. Lao, and S. Crotty. 2011. ICOS receptor instructs T follicular helper cell versus effector cell differentiation via induction of the transcriptional repressor Bcl6. *Immunity.* 34:932–946. <https://doi.org/10.1016/j.immuni.2011.03.023>
- Chyou, S., F. Benahmed, J. Chen, V. Kumar, S. Tian, M. Lipp, and T.T. Lu. 2011. Coordinated regulation of lymph node vascular-stromal growth first by CD11c+ cells and then by T and B cells. *J. Immunol.* 187:5558–5567. <https://doi.org/10.4049/jimmunol.1101724>
- Cohen, S., I.A. McGREGOR, and S. Carrington. 1961. Gamma-globulin and acquired immunity to human malaria. *Nature.* 192:733–737. <https://doi.org/10.1038/192733a0>
- Constant, S.L. 1999. B lymphocytes as antigen-presenting cells for CD4+ T cell priming in vivo. *J. Immunol.* 162:5695–5703.
- Corbo-Rodgers, E., K.R. Wiehagen, E.S. Staub, and J.S. Maltzman. 2012. Homeostatic division is not necessary for antigen-specific CD4+ memory T cell persistence. *J. Immunol.* 189:3378–3385. <https://doi.org/10.4049/jimmunol.1201583>
- Crompton, P.D., M.A. Kayala, B. Traore, K. Kayentao, A. Onoiba, G.E. Weiss, D.M. Molina, C.R. Burk, M. Waisberg, A. Jasinskias, et al. 2010. A prospective analysis of the Ab response to Plasmodium falciparum before and after a malaria season by protein microarray. *Proc. Natl. Acad. Sci. USA.* 107:6958–6963. <https://doi.org/10.1073/pnas.1001323107>
- Deenick, E.K., A. Chan, C.S. Ma, D. Gatto, P.L. Schwartzberg, R. Brink, and S.G. Tangye. 2010. Follicular helper T cell differentiation requires continuous antigen presentation that is independent of unique B cell signaling. *Immunity.* 33:241–253. <https://doi.org/10.1016/j.immuni.2010.07.015>
- DiToro, D., C.J. Winstead, D. Pham, S. Witte, R. Andargachew, J.R. Singer, C.G. Wilson, C.L. Zindl, R.J. Luther, D.J. Silberger, et al. 2018. Differential IL-2 expression defines developmental fates of follicular versus non-follicular helper T cells. *Science.* 361:eaao2933. <https://doi.org/10.1126/science.aao2933>
- Dow, C., C. Oseroff, B. Peters, C. Nance-Sotelo, J. Sidney, M. Buchmeier, A. Sette, and B.R. Mohle. 2008. Lymphocytic choriomeningitis virus infection yields overlapping CD4+ and CD8+ T-cell responses. *J. Virol.* 82:11734–11741. <https://doi.org/10.1128/JVI.00435-08>
- Dunn, R.J., E. Mertsching, R. Peach, and M. Kehry. 2007. Anti-mouse CD20 antibodies and uses thereof. World Intellectual Property Organization patent WO2007064911A1, filed December 4, 2006, and issued June 7, 2007.
- Evans, D.E., M.W. Munks, J.M. Purkerson, and D.C. Parker. 2000. Resting B lymphocytes as APC for naive T lymphocytes: dependence on CD40 ligand/CD40. *J. Immunol.* 164:688–697. <https://doi.org/10.4049/jimmunol.164.2.688>
- Fairfax, K.C., B. Everts, E. Amiel, A.M. Smith, G. Schramm, H. Haas, G.J. Randolph, J.J. Taylor, and E.J. Pearce. 2015. IL-4-secreting secondary T follicular helper (Tfh) cells arise from memory T cells, not persisting Tfh cells, through a B cell-dependent mechanism. *J. Immunol.* 194:2999–3010. <https://doi.org/10.4049/jimmunol.1401225>
- Fernandez-Ruiz, D., L.S. Lau, N. Ghazanfari, C.M. Jones, W.Y. Ng, G.M. Davey, D. Berthold, L. Holz, Y. Kato, M.H. Enders, et al. 2017. Development of a Novel CD4+ TCR Transgenic Line That Reveals a Dominant Role for CD8+ Dendritic Cells and CD40 Signaling in the Generation of Helper and CTL Responses to Blood-Stage Malaria. *J. Immunol.* 199:4165–4179. <https://doi.org/10.4049/jimmunol.1700186>
- Freitas do Rosário, A.P., S.M. Muxel, S.M. Rodríguez-Málaga, L.R. Sardinha, C.A. Zago, S.I. Castillo-Méndez, J.M. Alvarez, and M.R. D'Império Lima. 2008. Gradual decline in malaria-specific memory T cell responses leads to failure to maintain long-term protective immunity to Plasmodium chabaudi AS despite persistence of B cell memory and circulating antibody. *J. Immunol.* 181:8344–8355. <https://doi.org/10.4049/jimmunol.181.12.8344>
- Glatman Zaretsky, A., J.J. Taylor, I.L. King, F.A. Marshall, M. Mohrs, and E.J. Pearce. 2009. T follicular helper cells differentiate from Th2 cells in response to helminth antigens. *J. Exp. Med.* 206:991–999. <https://doi.org/10.1084/jem.20090303>
- Götz, A., M.S. Tang, M.C. Ty, C. Arama, A. Onoiba, D. Doumtabe, B. Traore, P.D. Crompton, P. Loke, and A. Rodriguez. 2017. Atypical activation of dendritic cells by Plasmodium falciparum. *Proc. Natl. Acad. Sci. USA.* 114:E10568–E10577. <https://doi.org/10.1073/pnas.1708383114>
- Gudmundsdottir, H., A.D. Wells, and L.A. Turka. 1999. Dynamics and requirements of T cell clonal expansion in vivo at the single-cell level: effector function is linked to proliferative capacity. *J. Immunol.* 162:5212–5223.
- Guermontprez, P., J. Helft, C. Claser, S. Deroubaix, H. Karanje, A. Gazumyan, G. Darasse-Jéze, S.B. Telerman, G. Breton, H.A. Schreiber, et al. 2013. Inflammatory Flt3l is essential to mobilize dendritic cells and for T cell responses during Plasmodium infection. *Nat. Med.* 19:730–738. <https://doi.org/10.1038/nm.3197>
- Hahn, W.O., N.S. Butler, S.E. Lindner, H.M. Akilesh, D.N. Sather, S.H. Kappe, J.A. Hamerman, M. Gale Jr., W.C. Liles, and M. Pepper. 2018. cGAS-mediated control of blood-stage malaria promotes Plasmodium-specific germinal center responses. *JCI Insight.* 3:e94142. <https://doi.org/10.1172/jci.insight.94142>
- Hale, J.S., B. Youngblood, D.R. Latner, A.U. Mohammed, L. Ye, R.S. Akondy, T. Wu, S.S. Iyer, and R. Ahmed. 2013. Distinct memory CD4+ T cells with commitment to T follicular helper- and T helper 1-cell lineages are generated after acute viral infection. *Immunity.* 38:805–817. <https://doi.org/10.1016/j.immuni.2013.02.020>
- Haque, A., S.E. Best, M. Montes de Oca, K.R. James, A. Ammerdorffer, C.L. Edwards, F. de Labastida Rivera, F.H. Amante, P.T. Bunn, M. Sheel, et al. 2014. Type I IFN signaling in CD8- DCs impairs Th1-dependent malaria immunity. *J. Clin. Invest.* 124:2483–2496. <https://doi.org/10.1172/JCI70698>
- Hawrylowicz, C.M., and E.R. Unanue. 1988. Regulation of antigen-presentation-I. IFN-gamma induces antigen-presenting properties on B cells. *J. Immunol.* 141:4083–4088.
- Haynes, N.M., C.D. Allen, R. Lesley, K.M. Ansel, N. Killeen, and J.G. Cyster. 2007. Role of CXCR5 and CCR7 in follicular Th cell positioning and appearance of a programmed cell death gene-high germinal center-associated subpopulation. *J. Immunol.* 179:5099–5108. <https://doi.org/10.4049/jimmunol.179.8.5099>
- Hirunpetcharat, C., J.H. Tian, D.C. Kaslow, N. van Rooijen, S. Kumar, J.A. Berzofsky, L.H. Miller, and M.F. Good. 1997. Complete protective immunity induced in mice by immunization with the 19-kilodalton carboxyl-terminal fragment of the merozoite surface protein-1 (MSPI [19]) of Plasmodium yoelii expressed in Saccharomyces cerevisiae: correlation of protection with antigen-specific antibody titer, but not with effector CD4+ T cells. *J. Immunol.* 159:3400–3411.
- Hondowicz, B.D., K.S. Kim, M.J. Ruterbusch, G.J. Keitany, and M. Pepper. 2018. IL-2 is required for the generation of viral-specific CD4+

- Th1 tissue-resident memory cells and B cells are essential for maintenance in the lung. *Eur. J. Immunol.* 48:80–86. <https://doi.org/10.1002/eji.201746928>
- Hong, S., Z. Zhang, H. Liu, M. Tian, X. Zhu, Z. Zhang, W. Wang, X. Zhou, F. Zhang, Q. Ge, et al. 2018. B Cells Are the Dominant Antigen-Presenting Cells that Activate Naive CD4⁺ T Cells upon Immunization with a Virus-Derived Nanoparticle Antigen. *Immunity.* 49:695–708.e4. <https://doi.org/10.1016/j.immuni.2018.08.012>
- Howland, K.C., L.J. Ausubel, C.A. London, and A.K. Abbas. 2000. The roles of CD28 and CD40 ligand in T cell activation and tolerance. *J. Immunol.* 164: 4465–4470. <https://doi.org/10.4049/jimmunol.164.9.4465>
- Itano, A.A., S.J. McSorley, R.L. Reinhardt, B.D. Ehst, E. Ingulli, A.Y. Rudensky, and M.K. Jenkins. 2003. Distinct dendritic cell populations sequentially present antigen to CD4 T cells and stimulate different aspects of cell-mediated immunity. *Immunity.* 19:47–57. [https://doi.org/10.1016/S1074-7613\(03\)00175-4](https://doi.org/10.1016/S1074-7613(03)00175-4)
- Iwata, A., V. Durai, R. Tussiwand, C.G. Briseño, X. Wu, G.E. Grajales-Reyes, T. Egawa, T.L. Murphy, and K.M. Murphy. 2017. Quality of TCR signaling determined by differential affinities of enhancers for the composite BATF-IRF4 transcription factor complex. *Nat. Immunol.* 18:563–572. <https://doi.org/10.1038/ni.3714>
- Johnston, R.J., A.C. Poholek, D. DiToro, I. Yusuf, D. Eto, B. Barnett, A.L. Dent, J. Craft, and S. Crotty. 2009. Bcl6 and Blimp-1 are reciprocal and antagonistic regulators of T follicular helper cell differentiation. *Science.* 325: 1006–1010. <https://doi.org/10.1126/science.1175870>
- Keck, S., M. Schmalzer, S. Ganter, L. Wyss, S. Oberle, E.S. Huseby, D. Zehn, and C.G. King. 2014. Antigen affinity and antigen dose exert distinct influences on CD4 T-cell differentiation. *Proc. Natl. Acad. Sci. USA.* 111: 14852–14857. <https://doi.org/10.1073/pnas.1403271111>
- Knowlden, Z.A., and A.J. Sant. 2016. CD4 T cell epitope specificity determines follicular versus non-follicular helper differentiation in the polyclonal response to influenza infection or vaccination. *Sci. Rep.* 6:28287. <https://doi.org/10.1038/srep28287>
- Krieger, J.I., S.F. Grammer, H.M. Grey, and R.W. Chesnut. 1985. Antigen presentation by splenic B cells: resting B cells are ineffective, whereas activated B cells are effective accessory cells for T cell responses. *J. Immunol.* 135:2937–2945.
- Krishnamoorthy, V., S. Kannanganat, M. Maienschein-Cline, S.L. Cook, J. Chen, N. Bahroos, E. Sievert, E. Corse, A. Chong, and R. Sciammas. 2017. The IRF4 Gene Regulatory Module Functions as a Read-Write Integrator to Dynamically Coordinate T Helper Cell Fate. *Immunity.* 47:481–497.e7. <https://doi.org/10.1016/j.immuni.2017.09.001>
- Langhorne, J., B. Simon-Haarhaus, and S.J. Meding. 1990. The role of CD4⁺ T cells in the protective immune response to *Plasmodium chabaudi* in vivo. *Immunol. Lett.* 25:101–107. [https://doi.org/10.1016/0165-2478\(90\)90099-C](https://doi.org/10.1016/0165-2478(90)90099-C)
- Loughland, J.R., G. Minigo, D.S. Sarovich, M. Field, P.E. Tipping, M. Montes de Oca, K.A. Pitera, F.H. Amante, B.E. Barber, M.J. Grigg, et al. 2017. Plasmacytoid dendritic cells appear inactive during sub-microscopic *Plasmodium falciparum* blood-stage infection, yet retain their ability to respond to TLR stimulation. *Sci. Rep.* 7:2596. <https://doi.org/10.1038/s41598-017-02096-2>
- Lu, K.T., Y. Kanno, J.L. Cannons, R. Handon, P. Bible, A.G. Elkhoulou, S.M. Anderson, L. Wei, H. Sun, J.J. O’Shea, and P.L. Schwartzberg. 2011. Functional and epigenetic studies reveal multistep differentiation and plasticity of in vitro-generated and in vivo-derived follicular T helper cells. *Immunity.* 35:622–632. <https://doi.org/10.1016/j.immuni.2011.07.015>
- MacLeod, M.K., A. McKee, F. Crawford, J. White, J. Kappler, and P. Marrack. 2008. CD4 memory T cells divide poorly in response to antigen because of their cytokine profile. *Proc. Natl. Acad. Sci. USA.* 105:14521–14526. <https://doi.org/10.1073/pnas.0807449105>
- Malleret, B., C. Claser, A.S. Ong, R. Suwanarusk, K. Sriprawat, S.W. Howland, B. Russell, F. Nosten, and L. Rénia. 2011. A rapid and robust tri-color flow cytometry assay for monitoring malaria parasite development. *Sci. Rep.* 1:118. <https://doi.org/10.1038/srep00118>
- Matloubian, M., R.J. Concepcion, and R. Ahmed. 1994. CD4⁺ T cells are required to sustain CD8⁺ cytotoxic T-cell responses during chronic viral infection. *J. Virol.* 68:8056–8063.
- McAdam, A.J., T.T. Chang, A.E. Lumelsky, E.A. Greenfield, V.A. Boussiotis, J.S. Duke-Cohan, T. Chernova, N. Malenkovich, C. Jabs, V.K. Kuchroo, et al. 2000. Mouse inducible costimulatory molecule (ICOS) expression is enhanced by CD28 costimulation and regulates differentiation of CD4⁺ T cells. *J. Immunol.* 165:5035–5040. <https://doi.org/10.4049/jimmunol.165.9.5035>
- McDonald, V., and R.S. Phillips. 1978. *Plasmodium chabaudi* in mice. Adoptive transfer of immunity with enriched populations of spleen T and B lymphocytes. *Immunology.* 34:821–830.
- Meredith, M.M., K. Liu, G. Darrasse-Jeze, A.O. Kamphorst, H.A. Schreiber, P. Guermonprez, J. Idoyaga, C. Cheong, K.H. Yao, R.E. Niec, and M.C. Nussenzweig. 2012. Expression of the zinc finger transcription factor zDC (Zbtb46, Btd4) defines the classical dendritic cell lineage. *J. Exp. Med.* 209:1153–1165. <https://doi.org/10.1084/jem.20112675>
- Moon, J.J., H.H. Chu, M. Pepper, S.J. McSorley, S.C. Jameson, R.M. Kedl, and M.K. Jenkins. 2007. Naive CD4⁺ T cell frequency varies for different epitopes and predicts repertoire diversity and response magnitude. *Immunity.* 27:203–213. <https://doi.org/10.1016/j.immuni.2007.07.007>
- Moss, D.K., E.J. Remarque, B.W. Faber, D.R. Cavanagh, D.E. Arnot, A.W. Thomas, and A.A. Holder. 2012. *Plasmodium falciparum* 19-kilodalton merozoite surface protein 1 (MSP1)-specific antibodies that interfere with parasite growth in vitro can inhibit MSP1 processing, merozoite invasion, and intracellular parasite development. *Infect. Immun.* 80: 1280–1287. <https://doi.org/10.1128/IAI.05887-11>
- Murphy, J.R. 1980. Host defenses in murine malaria: immunological characteristics of a protracted state of immunity to *Plasmodium yoelii*. *Infect. Immun.* 27:68–74.
- Nelson, R.W., D. Beisang, N.J. Tubo, T. Dileepan, D.L. Wiesner, K. Nielsen, M. Wüthrich, B.S. Klein, D.I. Kotov, J.A. Spanier, et al. 2015. T cell receptor cross-reactivity between similar foreign and self peptides influences naive cell population size and autoimmunity. *Immunity.* 42:95–107. <https://doi.org/10.1016/j.immuni.2014.12.022>
- Nurieva, R.I., Y. Chung, D. Hwang, X.O. Yang, H.S. Kang, L. Ma, Y.H. Wang, S.S. Watowich, A.M. Jetten, Q. Tian, and C. Dong. 2008. Generation of T follicular helper cells is mediated by interleukin-21 but independent of T helper 1, 2, or 17 cell lineages. *Immunity.* 29:138–149. <https://doi.org/10.1016/j.immuni.2008.05.009>
- Nurieva, R.I., Y. Chung, G.J. Martinez, X.O. Yang, S. Tanaka, T.D. Matsukevitch, Y.H. Wang, and C. Dong. 2009. Bcl6 mediates the development of T follicular helper cells. *Science.* 325:1001–1005. <https://doi.org/10.1126/science.1176676>
- Obeng-Adjei, N., S. Portugal, T.M. Tran, T.B. Yazew, J. Skinner, S. Li, A. Jain, P.L. Felgner, O.K. Doumbo, K. Kayentao, et al. 2015. Circulating Th1-Cell-type Tfh Cells that Exhibit Impaired B Cell Help Are Preferentially Activated during Acute Malaria in Children. *Cell Reports.* 13:425–439. <https://doi.org/10.1016/j.celrep.2015.09.004>
- Opat, M.M., V.H. Carpio, S.A. Ibitokou, B.E. Dillon, J.M. Obiero, and R. Stephens. 2015. Early effector cells survive the contraction phase in malaria infection and generate both central and effector memory T cells. *J. Immunol.* 194:5346–5354. <https://doi.org/10.4049/jimmunol.1403216>
- Oxenius, A., M.F. Bachmann, R.M. Zinkernagel, and H. Hengartner. 1998. Virus-specific MHC-class II-restricted TCR-transgenic mice: effects on humoral and cellular immune responses after viral infection. *Eur. J. Immunol.* 28:390–400. [https://doi.org/10.1002/\(SICI\)1521-4141\(199801\)28:01<390::AID-IMMU390>3.0.CO;2-O](https://doi.org/10.1002/(SICI)1521-4141(199801)28:01<390::AID-IMMU390>3.0.CO;2-O)
- Park, S.O., Y.W. Han, A.G. Aleyas, J.A. George, H.A. Yoon, J.H. Lee, H.Y. Kang, S.H. Kang, and S.K. Eo. 2008. Low-dose antigen-experienced CD4⁺ T cells display reduced clonal expansion but facilitate an effective memory pool in response to secondary exposure. *Immunology.* 123: 426–437. <https://doi.org/10.1111/j.1365-2567.2007.02707.x>
- Pepper, M., A.J. Pagan, B.Z. Igyártó, J.J. Taylor, and M.K. Jenkins. 2011. Opposing signals from the Bcl6 transcription factor and the interleukin-2 receptor generate T helper 1 central and effector memory cells. *Immunity.* 35:583–595. <https://doi.org/10.1016/j.immuni.2011.09.009>
- Pérez-Mazliah, D., D.H. Ng, A.P. Freitas do Rosário, S. McLaughlin, B. Mastelic-Gavillet, J. Sodenkamp, G. Kushinga, and J. Langhorne. 2015. Disruption of IL-21 signaling affects T cell-B cell interactions and abrogates protective humoral immunity to malaria. *PLoS Pathog.* 11:e1004715. <https://doi.org/10.1371/journal.ppat.1004715>
- Pinzon-Charry, A., T. Woodberry, V. Kienzle, V. McPhun, G. Minigo, D.A. Lampah, E. Kenangalem, C. Engwerda, J.A. López, N.M. Anstey, and M.F. Good. 2013. Apoptosis and dysfunction of blood dendritic cells in patients with *falciparum* and vivax malaria. *J. Exp. Med.* 210:1635–1646. <https://doi.org/10.1084/jem.20121972>
- Poholek, A.C., K. Hansen, S.G. Hernandez, D. Eto, A. Chandele, J.S. Weinstein, X. Dong, J.M. Odegard, S.M. Kaech, A.L. Dent, et al. 2010. In vivo regulation of Bcl6 and T follicular helper cell development. *J. Immunol.* 185: 313–326. <https://doi.org/10.4049/jimmunol.0904023>

- Qi, H., J.L. Cannons, F. Klauschen, P.L. Schwartzberg, and R.N. Germain. 2008. SAP-controlled T-B cell interactions underlie germinal centre formation. *Nature*. 455:764–769. <https://doi.org/10.1038/nature07345>
- Riley, E.M., S.J. Allen, J.G. Wheeler, M.J. Blackman, S. Bennett, B. Takacs, H.J. Schönfeld, A.A. Holder, and B.M. Greenwood. 1992. Naturally acquired cellular and humoral immune responses to the major merozoite surface antigen (PfMSP1) of *Plasmodium falciparum* are associated with reduced malaria morbidity. *Parasite Immunol.* 14:321–337. <https://doi.org/10.1111/j.1365-3024.1992.tb00471.x>
- Roberts, D.W., R.G. Rank, W.P. Weidanz, and J.F. Finerty. 1977. Prevention of recrudescence malaria in nude mice by thymic grafting or by treatment with hyperimmune serum. *Infect. Immunol.* 16:821–826.
- Rubtsov, A.V., K. Rubtsova, A. Fischer, R.T. Meehan, J.Z. Gillis, J.W. Kappler, and P. Marrack. 2011. Toll-like receptor 7 (TLR7)-driven accumulation of a novel CD11c⁺ B-cell population is important for the development of autoimmunity. *Blood*. 118:1305–1315. <https://doi.org/10.1182/blood-2011-01-331462>
- Salek-Ardakani, S., Y.S. Choi, M. Rafii-El-Idrissi Benhnia, R. Flynn, R. Arens, S. Shoenerberger, S. Crotty, M. Croft, and S. Salek-Ardakani. 2011. B cell-specific expression of B7-2 is required for follicular Th cell function in response to vaccinia virus. *J. Immunol.* 186:5294–5303. <https://doi.org/10.4049/jimmunol.1100406>
- Sallusto, F., D. Lenig, R. Förster, M. Lipp, and A. Lanzavecchia. 1999. Two subsets of memory T lymphocytes with distinct homing potentials and effector functions. *Nature*. 401:708–712. <https://doi.org/10.1038/44385>
- Satpathy, A.T., W. Kc, J.C. Albring, B.T. Edelson, N.M. Kretzer, D. Bhattacharya, T.L. Murphy, and K.M. Murphy. 2012. Zbtb46 expression distinguishes classical dendritic cells and their committed progenitors from other immune lineages. *J. Exp. Med.* 209:1135–1152. <https://doi.org/10.1084/jem.20120030>
- Stephens, R., and J. Langhorne. 2010. Effector memory Th1 CD4 T cells are maintained in a mouse model of chronic malaria. *PLoS Pathog.* 6:e1001208. <https://doi.org/10.1371/journal.ppat.1001208>
- Sullivan, R.T., C.C. Kim, M.F. Fontana, M.E. Feeney, P. Jagannathan, M.J. Boyle, C.J. Drakeley, I. Ssewanyana, F. Nankya, H. Mayanja-Kizza, et al. 2015. FCRL5 Delineates Functionally Impaired Memory B Cells Associated with *Plasmodium falciparum* Exposure. *PLoS Pathog.* 11:e1004894. <https://doi.org/10.1371/journal.ppat.1004894>
- Tran, T.M., S. Li, S. Doumbo, D. Doumtable, C.-Y. Huang, S. Dia, A. Bathily, J. Sangala, Y. Kone, A. Traore, et al. 2013. An intensive longitudinal cohort study of Malian children and adults reveals no evidence of acquired immunity to *Plasmodium falciparum* infection. *Clin. Infect. Dis.* 57:40–47. <https://doi.org/10.1093/cid/cit174>
- Tube, N.J., A.J. Pagán, J.J. Taylor, R.W. Nelson, J.L. Linehan, J.M. Ertelt, E.S. Huseby, S.S. Way, and M.K. Jenkins. 2013. Single naive CD4⁺ T cells from a diverse repertoire produce different effector cell types during infection. *Cell*. 153:785–796. <https://doi.org/10.1016/j.cell.2013.04.007>
- Ueffing, K., H. Abberger, A.M. Westendorf, K. Matuschewski, J. Buer, and W. Hansen. 2017. Conventional CD11c^{high} dendritic cells are important for T cell priming during the initial phase of *Plasmodium yoelii* infection, but are dispensable at later time points. *Front. Immunol.* 8:1333. <https://doi.org/10.3389/fimmu.2017.01333>
- Urban, B.C., D.J. Ferguson, A. Pain, N. Willcox, M. Plebanski, J.M. Austyn, and D.J. Roberts. 1999. *Plasmodium falciparum*-infected erythrocytes modulate the maturation of dendritic cells. *Nature*. 400:73–77. <https://doi.org/10.1038/21900>
- Urban, B.C., T.T. Hien, N.P. Day, N.H. Phu, R. Roberts, E. Pongponratn, M. Jones, N.T. Mai, D. Bethell, G.D. Turner, et al. 2005. Fatal *Plasmodium falciparum* malaria causes specific patterns of splenic architectural disorganization. *Infect. Immunol.* 73:1986–1994. <https://doi.org/10.1128/IAI.73.4.1986-1994.2005>
- Urban, B.C., D. Cordery, M.J. Shafi, P.C. Bull, C.I. Newbold, T.N. Williams, and K. Marsh. 2006. The frequency of BDCA3-positive dendritic cells is increased in the peripheral circulation of Kenyan children with severe malaria. *Infect. Immunol.* 74:6700–6706. <https://doi.org/10.1128/IAI.00861-06>
- Voisine, C., B. Mastelic, A.M. Sponaas, and J. Langhorne. 2010. Classical CD11c⁺ dendritic cells, not plasmacytoid dendritic cells, induce T cell responses to *Plasmodium chabaudi* malaria. *Int. J. Parasitol.* 40:711–719. <https://doi.org/10.1016/j.ijpara.2009.11.005>
- Watanabe, M., C. Fujihara, A.J. Radtke, Y.J. Chiang, S. Bhatia, R.N. Germain, and R.J. Hodes. 2017. Co-stimulatory function in primary germinal center responses: CD40 and B7 are required on distinct antigen-presenting cells. *J. Exp. Med.* 214:2795–2810. <https://doi.org/10.1084/jem.20161955>
- Weinbaum, F.I., C.B. Evans, and R.E. Tigelaar. 1976. Immunity to *Plasmodium Berghei yoelii* in mice. I. The course of infection in T cell and B cell deficient mice. *J. Immunol.* 117:1999–2005.
- Weiss, G.E., P.D. Crompton, S. Li, L.A. Walsh, S. Moir, B. Traore, K. Kayentao, A. Ongoiba, O.K. Doumbo, and S.K. Pierce. 2009. Atypical memory B cells are greatly expanded in individuals living in a malaria-endemic area. *J. Immunol.* 183:2176–2182. <https://doi.org/10.4049/jimmunol.0901297>
- Whitmire, J.K., N. Benning, and J.L. Whitton. 2006. Precursor frequency, nonlinear proliferation, and functional maturation of virus-specific CD4⁺ T cells. *J. Immunol.* 176:3028–3036. <https://doi.org/10.4049/jimmunol.176.5.3028>
- Woodberry, T., G. Minigo, K.A. Piera, F.H. Amante, A. Pinzon-Charry, M.F. Good, J.A. Lopez, C.R. Engwerda, J.S. McCarthy, and N.M. Anstey. 2012. Low-level *Plasmodium falciparum* blood-stage infection causes dendritic cell apoptosis and dysfunction in healthy volunteers. *J. Infect. Dis.* 206:333–340. <https://doi.org/10.1093/infdis/jis366>
- World Health Organization. 2018. World Malaria Report 2018. Available at: <https://www.who.int/malaria/publications/world-malaria-report-2018/en/> (accessed Month Day, Year)
- Wu, T., H.M. Shin, E.A. Moseman, Y. Ji, B. Huang, C. Harly, J.M. Sen, L.J. Berg, L. Gattinoni, D.B. McGavern, and P.L. Schwartzberg. 2015. TCF1 Is Required for the T Follicular Helper Cell Response to Viral Infection. *Cell Reports*. 12:2099–2110. <https://doi.org/10.1016/j.celrep.2015.08.049>
- Wykes, M.N., X.Q. Liu, L. Beattie, D.I. Stanicic, K.J. Stacey, M.J. Smyth, R. Thomas, and M.F. Good. 2007. *Plasmodium* strain determines dendritic cell function essential for survival from malaria. *PLoS Pathog.* 3:e96. <https://doi.org/10.1371/journal.ppat.0030096>
- Zander, R.A., R. Vijay, A.D. Pack, J.J. Guthmiller, A.C. Graham, S.E. Lindner, A.M. Vaughan, S.H.I. Kappe, and N.S. Butler. 2017. Th1-like *Plasmodium*-Specific Memory CD4⁺ T Cells Support Humoral Immunity. *Cell Reports*. 21:1839–1852. <https://doi.org/10.1016/j.celrep.2017.10.077>

Supplemental material

Arroyo et al., <https://doi.org/10.1084/jem.20190849>

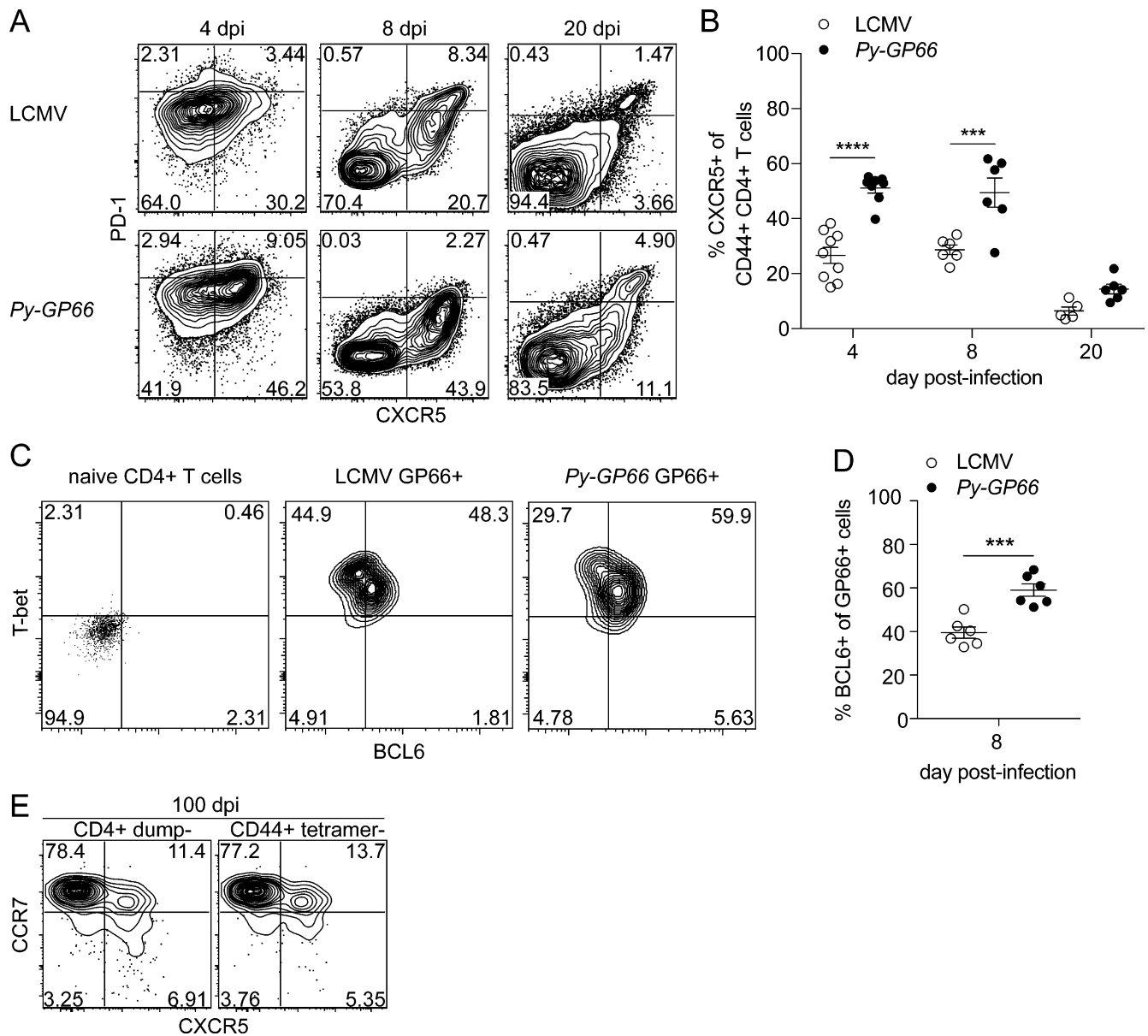


Figure S1. **The global CD4⁺ T cell response to Py-GP66 is skewed toward a Tfh phenotype.** (A) Representative flow plots of CD44⁺ antigen-nonspecific cells from acute time points with LCMV or Py-GP66 in WT mice. Cells are gated on dump⁻ CD3⁺ CD8⁻ CD4⁺ CD44⁺ cells. (B) Summary data of the percentage of CXCR5⁺ cells from A. Data are pooled from five to nine mice per cohort and are representative of two independent experiments. Data were analyzed by two-way ANOVA. (C) Representative plots of naive cells (gated on dump⁻ CD3⁺ CD8⁻ CD4⁺ CD44⁻) and the LCMV and Py-GP66 plots (gated on dump⁻ CD3⁺ CD8⁻ CD4⁺ CD44⁺ GP66⁺) show T-bet and BCL6 expression 8 d after infection with LCMV and Py-GP66 infection. (D) Summary data of the percentage of BCL6⁺ GP66⁺ cells from C. Data are pooled from six mice per cohort and are representative of two independent experiments. Data were analyzed by unpaired t test. (E) Plots are gated on dump⁻ CD3⁺ CD8⁻ CD4⁺ cells and dump⁻ CD3⁺ CD8⁻ CD4⁺ CD44⁺ GP66⁻ cells, respectively, following 100 d of Py-GP66 infection. Representative of six mice from at least two independent experiments. For B and D, data are shown as means ± SEM. ***, P < 0.001; ****, P < 0.0001. ns, not significant.

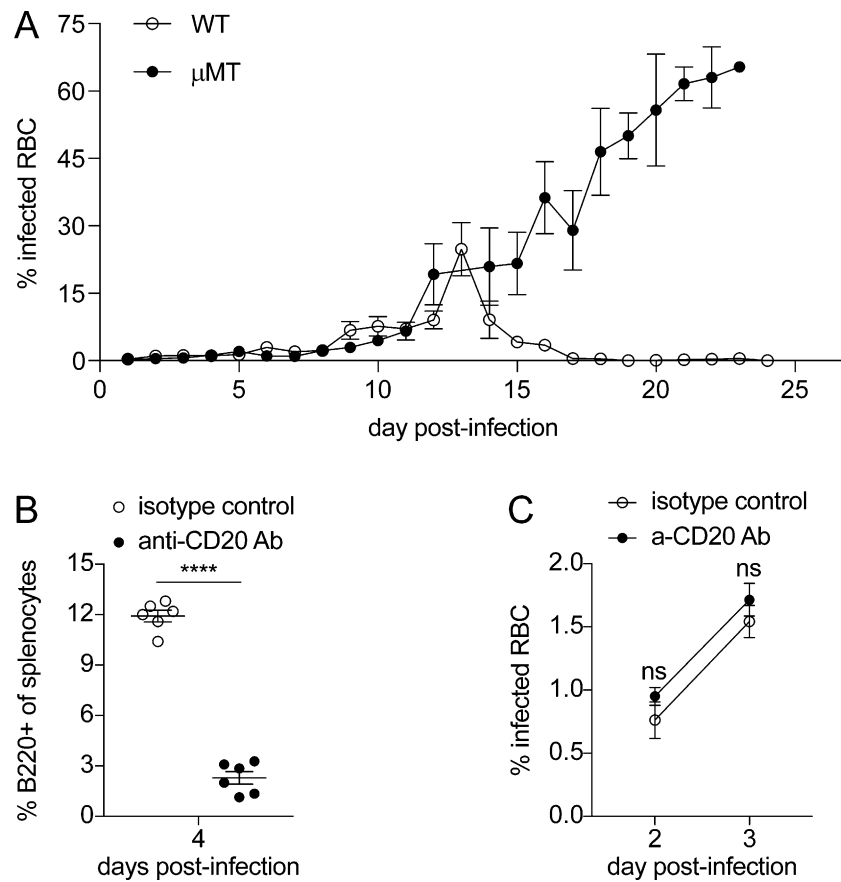


Figure S2. **A lack of B cells does not impact early parasite burden.** **(A)** Percentage of infected red blood cells in WT and μ MT mice following *Py-GP66* infection. Data are pooled from 3–21 mice per cohort and are representative of over two independent experiments. **(B)** Percentage of B220⁺ B cells following anti-CD20 depletion and 4 d of *Py-GP66* infection. Data are pooled from six mice per cohort and are representative of two independent experiments. Data were analyzed by unpaired *t* test. **(C)** Percentage of infected red blood cells in WT mice treated with anti-CD20 antibody or isotype control. Data are pooled from six mice per cohort and are representative of two independent experiments. Data were analyzed by two-way ANOVA. For A–C, data are shown as means \pm SEM. ****, $P < 0.0001$. Ab, antibody; ns, not significant.

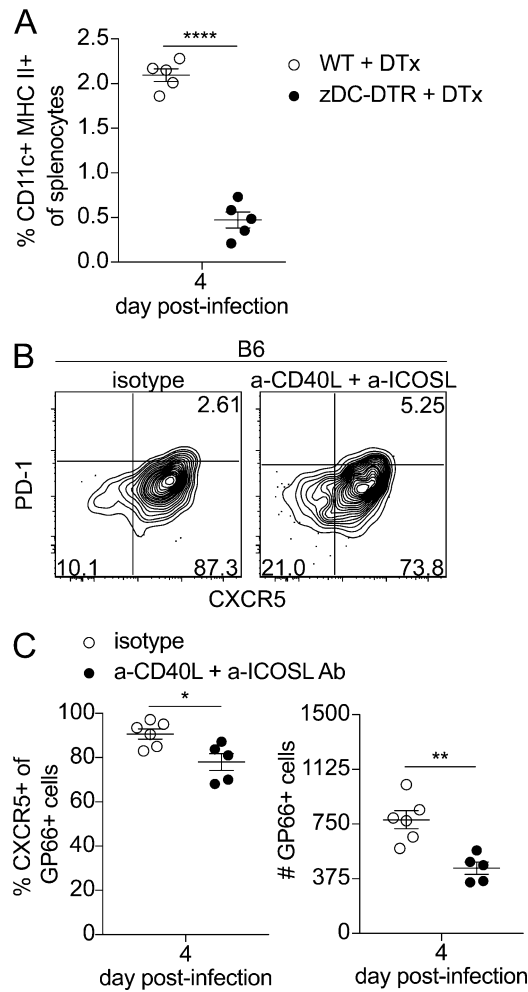


Figure S3. **Costimulatory signal blockade in WT mice results in a decreased Tfh response.** **(A)** Percentage of CD11c⁺ MHC II⁺ cells following diphtheria toxin treatment (DTx) in WT and zDC-DTR mice. Data are pooled from five mice per cohort and are representative of two independent experiments. Data were analyzed by unpaired *t* test. **(B)** WT mice were treated with a-CD40L + a-ICOSL antibodies or isotype controls daily 0–3 d after infection. Representative flow plots are from GP66⁺ cells 4 d after infection with *Py-GP66*. **(C)** Summary data of the percentage of CXCR5⁺ GP66⁺ cells and number of GP66⁺ cells from A. Data are pooled from five or six mice per cohort and are representative of two independent experiments. Data were analyzed by unpaired *t* test. For A and C, data are shown as means ± SEM. *, *P* < 0.05; **, *P* < 0.01; ****, *P* < 0.0001.